Contribution from the Max-Planck-Institut für Festkörperforschung, 7000 Stuttgart 80, West Germany

Structural Separation of Rubidium and Cesium in an Alkali Metal Suboxide

ARNDT SIMON,* WULF BRÄMER, and HANS-JÖRG DEISEROTH

Received August 9, 1977

Partial oxidation of rubidium–cesium alloys leads to the formation of ternary suboxides. The compound $Rb_7Cs_{11}O_3$ is the first of a series of compounds to be isolated and investigated. The compound is prepared by reacting stoichiometric amounts of the elements; oxygen is introduced by thermal decomposition of mercury oxide. $Rb_7Cs_{11}O_3$ forms needle-shaped metallic crystals of violet-bronze color melting at −21.9 °C. Single crystals have been grown in an automated single-crystal diffractometer and investigated at −90 °C using Mo Kα radiation. The compound crystallizes in the orthorhombic space group $P2_12_12_1$ (No. 19) with a_0 = 3228.12 (10) pm, b_0 = 2187.7 (7) pm, c_0 = 902.5 (4) pm, and Z = 4. The structure has been refined to a conventional residual R = 0.073 and R_w = 0.077 including 969 observed reflections. It contains clusters of composition $Cs_{11}O_3$ which also occur in the binary cesium suboxides. The oxygen atom is surrounded by a distorted octahedron of Cs atoms. The $Cs_{11}O_3$ cluster is formed by three octahedra sharing faces. Within the limits of the experiment only cesium atoms belong to the ion clusters. The rubidium atoms are arranged in close-packed wavy sheets filling the space between columns of $Cs_{11}O_3$ clusters. According to the spectrum of interatomic distances, chemical bonding within the clusters is predominantly ionic, whereas bonding between the clusters and between the rubidium atoms is purely metallic. The electronic properties of $Rb_7Cs_{11}O_3$ have been investigated (UV PES) and discussed with respect to the crystal structure.

Introduction

Metal-rich oxides of the heavy alkali metals rubidium and cesium have been extensively studied during the last few years.[1,2] These compounds follow a unique structure pattern, the essence of which is the occurrence of ion clusters with metallic type of bonding between them. In the case of rubidium, the characteristic Rb_9O_2 cluster, which is formed by face sharing of two Rb octahedra centered by oxygen atoms, is found. This atomic arrangement is well-known from the anti-type ion $M_2Cl_9^{3-}$. The copper-red compound Rb_9O_2 consists only of such clusters, well separated from one another.[3] In the case of cesium, face sharing of three oxygen-centered Cs octahedra leads to the trigonal $Cs_{11}O_3$ cluster, which is the only constituent of the compound $Cs_{11}O_3$.[4] The compounds Rb_9O_2 and $Cs_{11}O_3$ react with stoichiometric amounts of alkali metal to form Rb_6O ($Rb_3Rb_9O_2$[5]), Cs_7O ($Cs_{10}Cs_{11}O_3$[6]) and Cs_4O ($CsCs_{11}O_3$[7]).

The structures of these compounds very clearly reflect the intermediate position of the alkali metal suboxides between salts and metals. The different bonding types are dominant in different parts of the structures. Of course, this leads to the question of whether the constituents of the different bonding regions can be substituted. This question has been followed by investigation of the oxidation behavior of Rb/Cs and K/Cs alloys. In both systems the existence of mixed-metal suboxides has been established.[8] Further investigations of the K/Cs/O system are extremely complicated due to the formation of K_2O at temperatures higher than −60 °C on the one hand and formation of hitherto unknown intermetallic phases (K_2Cs, K_7Cs_6[9]) at temperatures below −90 °C on the other hand. These difficulties do not occur in the Rb/Cs/O system. Nevertheless investigations in this system are difficult mainly because of a pronounced delay of compound formation due to kinetics.

In this paper we report on the first Rb/Cs-mixed suboxide of composition $Rb_7Cs_{11}O_3$.

Experimental Section

Preparation. The compound $Rb_7Cs_{11}O_3$ is prepared by reacting a suitable Rb/Cs alloy with a stoichiometric amount of oxygen (a) or by adding the stoichiometric amount of rubidium to $Cs_{11}O_3$ (b). Experimental details were given in previous papers.[9,10] The metals were prepared by the Hackspill method using p.a. quality RbCl and CsCl (less than 0.01% Cs and Rb, respectively) and Ca (less than 0.01% alkali metal, mainly Na).[10]

(a) In a special run 6.1 g of Cs and 2.4 g of Rb were mixed in a thoroughly degassed glass vessel under Ar. The quantity of the second metal added could be determined with an accuracy of ±0.05 g; the exact amount was determined by reweighing.[9,10] Purification of the inert gas was achieved by passing it through molecular sieves, through columns with P_2O_5, and then over porous Ti at 700 °C and finally by bubbling the gas through a liquid Na/K alloy. After the complete apparatus had been evacuated to 10^{-5} Torr, the oxygen was introduced by thermal decomposition of 2.67 g of HgO, which had been prepared by combination of the elements.[11] The mercury was deposited in a cold trap, surrounded by acetone/dry ice, and the oxygen was slowly reacted with Rb/Cs alloy using a magnetic stirrer. The mercury was recovered quantitatively. A contamination of the alkali metal by Hg could be excluded, as a piece of gold foil in the gas inlet system of the reaction vessel did not contain a detectable amount of Hg after the oxidation reaction.[10] As no loss of alkali metal occurred and since the final pressure was below 10^{-3} Torr, a chemical analysis of the reaction product was unnecessary.

(b) Samples of variable composition $Rb_xCs_{11}O_3$ were prepared by first oxidizing Cs to $Cs_{11}O_3$ and successively adding liquid Rb.

In the case of the composition $Rb_7Cs_{11}O_3$, procedure (a) as well as (b) leads to a bronze-colored melt with a slightly violet tinge, which solidifies congruently at −21.9 °C to form needle-shaped crystals. These are as sensitive to oxygen and moisture as the metals themselves. They ignite spontaneously in air and react explosively with water.

Phase Analysis. Because of the quantitative reaction between Rb and Cs with O_2, the sample compositions are well defined. This makes chemical analysis of the whole bulk unnecessary. Thermal analyses have been carried out in a special DTA apparatus described elsewhere[9] (accuracy of temperature registration ±0.02 °C; rate of heating 15 °C/h).

Polycrystalline samples have been investigated by the modified Guinier technique[12] using glass capillaries of 0.1-mm diameter and silicon as a standard[13] attached to the outside of the capillary (a = 543.06 pm at room temperature, $\alpha = 2.7 \times 10^{-6}$,[14] λ 154.051 pm, camera diameter 114.6 mm). To avoid effects due to preferred crystallite orientations, the liquid samples must be rapidly quenched from room temperature to −150 °C in the camera. This procedure normally yielded amorphous samples. Therefore the samples had been annealed at −50 °C for some hours before x-ray investigation was started.

Single crystals of $Rb_7Cs_{11}O_3$ have been grown in a diffractometer (see below) by the capillary method.[1,7,9] A capillary of 0.1-mm diameter was filled with the liquid sample to a height of 30 mm and attached to the diffractometer (see below) equipped with a low-temperature device.[6] The capillary was surrounded by a metal screen (held at ca. +30 °C). Part of the capillary reached into a cold nitrogen gas stream through a central hole (diameter 0.3 mm) of the screen. The equipment used has been described in more detail elsewhere.[7] Nutrient formation was achieved at −100 °C (pronounced supersaturation). Suitable single crystals for x-ray investigations were grown then by slowly moving the metal screen, thus introducing the complete capillary into the gas stream blowing at −25 °C. In several attempts the [001] direction of the crystals was found to be aligned parallel to the capillary axis. As $Rb_7Cs_{11}O_3$ exhibits a range of homogeneity

0020-1669/78/1317-0875$01.00/0

Table I. Final Atomic Parameters[a] for $Rb_7Cs_{11}O_3$ in Space Group $P2_12_12_1$ (D_2^4) (Standard Deviations in Parentheses)

Atom	G	x	y	z	U_{11}	U_{22}	U_{33}	U_{12}	U_{13}	U_{23}
Cs1	1.00 (2)	4130 (4)	1959 (4)	−2063 (10)	0.069 (8)	0.103 (5)	0.118 (6)	0.007 (7)	0.010 (7)	0.000 (5)
Cs2	0.98 (2)	4120 (3)	1975 (4)	2043 (10)	0.064 (8)	0.089 (6)	0.112 (5)	−0.003 (7)	0.005 (6)	0.012 (5)
Cs3	1.03 (2)	4166 (6)	57 (6)	−2136 (18)	0.149 (13)	0.106 (9)	0.282 (15)	−0.008 (12)	0.009 (14)	−0.085 (10)
Cs4	0.99 (2)	4173 (6)	98 (6)	2281 (18)	0.207 (14)	0.121 (8)	0.243 (16)	0.020 (12)	0.023 (14)	0.074 (10)
Cs5	0.97 (2)	3008 (4)	2882 (7)	−2240 (13)	0.062 (8)	0.158 (9)	0.161 (9)	0.024 (8)	−0.035 (8)	−0.008 (8)
Cs6	1.01 (2)	2989 (4)	2857 (7)	2241 (13)	0.072 (9)	0.119 (10)	0.154 (8)	0.026 (9)	0.022 (8)	−0.025 (8)
Cs7	1.01 (2)	5203 (4)	2940 (7)	−2278 (15)	0.113 (14)	0.168 (10)	0.176 (10)	−0.052 (9)	0.047 (10)	0.019 (9)
Cs8	0.99 (2)	5212 (3)	2975 (8)	2175 (15)	0.065 (10)	0.142 (13)	0.188 (10)	−0.011 (9)	−0.022 (9)	−0.021 (10)
Cs9	0.99 (1)	3273 (2)	1192 (3)	6 (22)	0.053 (5)	0.106 (4)	0.196 (7)	−0.026 (3)	0.023 (10)	−0.013 (10)
Cs10	1.00 (1)	4093 (2)	3455 (2)	32 (15)	0.079 (5)	0.068 (3)	0.163 (6)	0.001 (3)	−0.008 (10)	−0.002 (6)
Cs11	0.99 (1)	5008 (2)	1260 (2)	18 (18)	0.059 (5)	0.096 (4)	0.175 (6)	0.020 (3)	−0.001 (9)	0.012 (8)
Rb1	0.99 (2)	1740 (3)	1391 (5)	69 (31)	0.072 (9)	0.128 (8)	0.220 (14)	−0.012 (6)	0.038 (15)	−0.029 (15)
Rb2	1.05 (2)	2840 (3)	5276 (3)	−15 (24)	0.063 (8)	0.090 (5)	0.180 (10)	0.001 (5)	−0.012 (13)	0.011 (11)
Rb3	0.99 (2)	2588 (3)	700 (4)	4990 (27)	0.117 (9)	0.106 (6)	0.159 (9)	−0.017 (6)	0.035 (16)	0.041 (15)
Rb4	1.00 (2)	4030 (4)	4415 (4)	4962 (30)	0.188 (12)	0.103 (6)	0.179 (11)	−0.002 (7)	−0.020 (20)	−0.016 (15)
Rb5	1.01 (1)	1591 (3)	3640 (4)	15 (30)	0.066 (8)	0.123 (7)	0.204 (12)	0.015 (6)	0.021 (17)	0.026 (16)
Rb6	1.02 (2)	1569 (3)	2397 (5)	5009 (35)	0.071 (8)	0.151 (8)	0.182 (11)	0.005 (6)	−0.018 (16)	−0.002 (16)
Rb7	0.99 (2)	4374 (3)	5718 (4)	−69 (26)	0.097 (9)	0.117 (7)	0.157 (9)	−0.012 (6)	0.016 (16)	0.029 (14)
O1		4196 (15)	932 (16)	206 (120)	0.063 (44)	0.031 (20)	0.318 (59)	−0.029 (24)	−0.129 (47)	0.089 (48)
O2		3459 (16)	2478 (24)	155 (104)	0.083 (45)	0.145 (40)	0.071 (37)	−0.009 (34)	−0.054 (55)	−0.026 (52)
O3		4704 (11)	2516 (15)	−73 (89)	0.007 (29)	0.047 (19)	0.083 (29)	−0.011 (18)	−0.016 (45)	−0.008 (36)

[a] Positional parameters are listed $\times 10^4$ and thermal parameters $\times 10^2$.[15] Lattice parameters: $a = 3228.2$ (10), $b = 2187.7$ (7), $c = 902.5$ (4) pm (−50 °C), modified Guinier technique.

(refer to Results), difficulties may occur due to the compositional changes within the growing single crystal. Therefore an exact sample composition was of great importance to avoid these difficulties as well as twinning or polycrystal formation. The special sample taken for crystal growth had a composition of 52.97 atom % Cs, 32.76 atom % Rb, and 14.26 atom % O corresponding to the formula $Rb_{6.89}Cs_{11.14}O_3$.

Data Collection and Reduction. X-ray data have been collected using an automated four-circle diffractometer *P*21 (Syntex). In addition to the special low-temperature device,[6] the instrument was equipped with an extra x-ray tube and an image intensifier tube for direct observation of Laue patterns. This provided a quick search for optimal crystal position along the capillary. The data set was recorded at −90 °C on the basis of an orthorhombic unit cell with $a = 3228$, $b = 2188$, and $c = 902$ pm. These data compared well with values derived from the modified Guinier technique at −50 °C, which are listed in Table I. Data were collected in the ω-scan mode (scans at 1–29.3°/min with ω divided into 19 steps; peak-to-background time ratio of 2; background measurements at $\Delta\omega = 1.2°$ off the peak center), using Mo Kα radiation within the range $3° \leq 2\theta \leq 45°$. Two standard peaks were monitored between every 18 reflections to check crystal and instrument stability.

To ensure a reliable data set, two differently grown crystals of the same sample were investigated. The better one was used for the refinement. The set of 3811 independently measured intensities still contained a number of incorrect data, mainly due to additional background from polycrystalline portions of the sample. All intensities with background measurements differing by a factor of 3 were eliminated leading to the final data set of 2912 reflections. Out of these, 969 reflections were observed with $I > 3\sigma(I)$. The large number of unobserved reflections was caused by the rapid decrease of intensities as a function of 2θ due to the very high Debye–Waller factors. After correction for polarization—Lorentz effect, these data were used for refinement without further corrections.

Structure Determination and Refinement. The calculations were carried out with a Nova 1200 minicomputer using the XTL-System (Syntex) and subsequently by using the x-ray system (Version 72)[15] at the computer center of the Max-Planck-Institut für Festkörperforschung.

The only systematic absences, $h \neq 2n$, $k \neq 2n$, and $l \neq 2n$, led to the space group $P2_12_12_1$. The characteristic length of the *c* axis, as in Cs_7O,[6] suggested the occurrence of the same $Cs_{11}O_3$ clusters with a similar orientation in $Rb_7Cs_{11}O_3$. At this stage volume considerations confirmed the assumed composition of this compound (refer to Results). The structure could be solved via the projection (*hk*0) by arranging $Cs_{11}O_3$ clusters in the plane group symmetry *pgg* in a way to give the highest intensities to the (350) and (810) reflections as observed. One of the models was refined to $R = 0.35$ and allowed the location of all Rb positions from the subsequent electron density map. Finally, this model could be refined to $R = 0.09$ (using 58 observed (*hk*0) reflections). Starting from the refined projection, one of the three-dimensional models was converging to a final unweighted residual $R = \sum||F_o| - |F_c||/\sum|F_o| = 0.073$ after several cycles of full-matrix least-squares refinement with anisotropic temperature factors; the weighted residual was $R_w = [\sum w(|F_o| - |F_c|)^2/\sum w|F_o|^2]^{0.5} = 0.077$ and the (unweighted) value including the unobserved reflection was $R' = 0.132$. Considerable difficulties arose from the large number of quasi-special atomic coordinates. Variation of the occupancy factors of Rb and Cs atoms did not indicate a significant deviation from unity. Thus the stoichiometric nature as well as a lack of mutual replacement of Rb and Cs atoms is clearly established for the special sample investigated. The final difference Fourier synthesis turned out to be flat to ±1 e/Å^3. Only the immediate neighborhood of the metal positions showed deviations of ±3 e/Å^3.

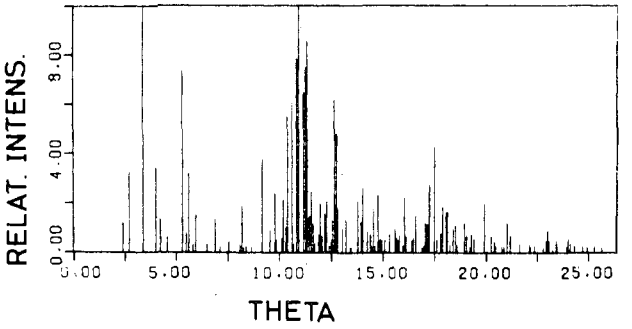

Figure 1. Calculated powder diffraction plot for the compound $Rb_7Cs_{11}O_3$ accepting the resolution of a Guinier photograph (λ 154.051 pm, $R = 57.3$ mm, $B = 0$).

Table I summarizes the structural data. The comparison between observed and calculated structure factors is available as supplementary material. For the purpose of characterizing $Rb_7Cs_{11}O_3$, the powder pattern as calculated with the final parameters ($B = 0$) according to the resolution of a Guinier diagram is reproduced in Figure 1.

Results

$Rb_7Cs_{11}O_3$ and the Neighboring Phases. The structure principle of the binary alkali metal suboxides—ion clusters introduced into a matrix of excess metal—suggests a variety of new compounds to occur in the Cs/Rb/O system. Yet there has been no conclusive answer to the question of whether the Rb_9O_2 or the $Cs_{11}O_3$ cluster was the more stable one in the mixed system. The somewhat smaller value of the ionization energy[16] for Cs (89.4 kcal/g-atom) as compared with the value for Rb (95.9 kcal/g-atom) favors cesium to be the constituent

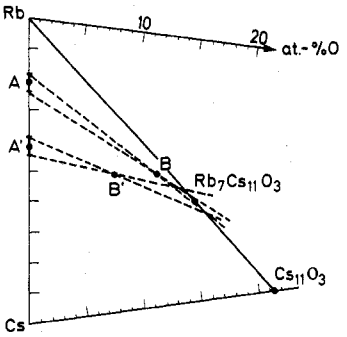

Figure 2. Ternary diagram for the $Rb/Cs/Cs_{11}O_3$ system. Solidification of phase compositions B and B′ lead to the formation of the coexisting mixed crystals A and A′ (bars indicate the accuracy of the determination of the alloy compositions). The compound composition $Rb_xCs_{11}O_3$ ($x \approx 7$) is found by extrapolating $\overline{AB}$ and $\overline{A'B'}$.

of the ionic clusters. But this effect could well be overcompensated by the higher value of the Coulomb energy due to smaller ion distances in the case of Rb. In this respect one has to keep in mind the deposition of solid Na_2O from a K/Na alloy during oxidation.[17]

By anticipating the same kind of clusters as in the binary systems, the stability of the clusters toward the alternate metal can easily be proved: (a) If the Rb_9O_2 cluster is stable in Cs, the addition of a large excess of Cs to Rb_9O_2 should result in the formation of a suboxide $Cs_xRb_9O_2$ coexisting with unreacted *pure Cs*. Similar conditions hold for the system $Cs_{11}O_3/Rb$; e.g., $Rb_9O_2 + xCs = Cs_yRb_9O_2 + (x-y)Cs$. (b) Instability of the Rb_9O_2 cluster in the same experiment would result in the formation of a suboxide of the kind $Cs_yRb_zCs_{11}O_3$ which then must be accompanied by a *Rb/Cs mixed crystal* (similar assumptions are valid in the case of instability of the $Cs_{11}O_3$ clusters toward Rb); e.g., $3Rb_9O_2 + xCs = 2Cs_yRb_zCs_{11}O_3 + Rb_{27-2z}Cs_{x-2y-22}$. In such sense the occurrence of pure Cs(Rb) or mixed Rb/Cs crystals provides a sensitive proof for the stability of the Rb_9O_2 and $Cs_{11}O_3$ clusters.

According to our experimental results, the Rb_9O_2 cluster is unstable in a system containing the elements Cs and O in an atomic ratio Cs:O > 11:3. At least in the solid state the pure $Cs_{11}O_3$ cluster is the only stable configuration within the compositional triangle between the limiting phases Rb, Cs, and $Cs_{11}O_3$ in the ternary Rb/Cs/O system. This triangle is drawn with respect to the adjacent binary systems in Figure 2.

Along the $Rb/Cs_{11}O_3$ line, suboxides of the general formula $Rb_xCs_{11}O_3$ coexist beside one another or pure Rb. Solid samples within the Rb-rich part of the triangle (atomic ratio Rb:Cs > 0.4) consist of Rb/Cs mixed crystals together with the stoichiometric suboxide $Rb_7Cs_{11}O_3$. Again the composition of the mixed crystals serves as an aid to localize the stoichiometry of the coexisting suboxide. As drawn in Figure 2, mixed crystals of compositions A′ and A are found with solidified samples B′ and B, which coexist with an identical suboxide characterized by its complicated x-ray pattern. Lines AB and A′B′ extrapolate fairly well to the composition $Rb_7Cs_{11}O_3$ even if rather large deviations in the determination of the mixed-crystal compositions indicated by bars are taken into account.

These results have been verified by systematic investigations along the $Cs_{11}O_3/Rb$ line by adding weighed amounts of metal to $Cs_{11}O_3$. Thermal analyses and x-ray investigations led to the phase relationships plotted in Figure 3(b). Besides the fact that temperatures of melting and decomposition of phases are lower in the $Cs_{11}O_3/Rb$ system, the main character of phase relationships compares very well with the binary $Cs_{11}O_3/Cs$ system (Figure 3(a)).

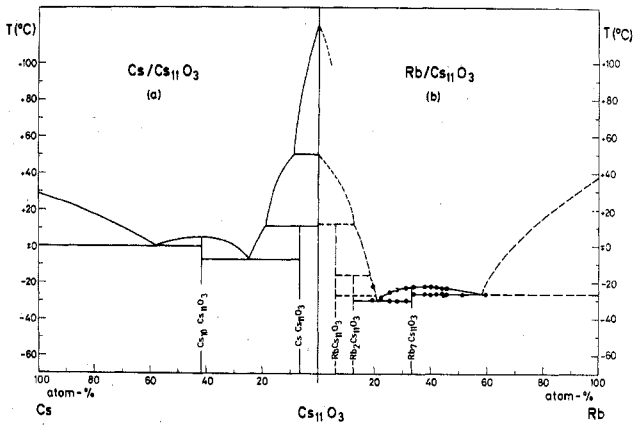

Figure 3. Comparison of thermal behavior of (a) $Cs/Cs_{11}O_3$ and (b) $Rb/Cs_{11}O_3$ mixtures. Temperatures of thermal effects are represented by dots.

$Rb_7Cs_{11}O_3$ corresponds to the binary compound $Cs_{10}Cs_{11}O_3$ (Cs_7O). Both compounds are the only alkali metal suboxides which melt congruently. The melting point of $Rb_7Cs_{11}O_3$ is found to be −21.9 °C. There is strong evidence for the existence of at least two more suboxides of the type $Rb_xCs_{11}O_3$. The structure of the incongruently melting compound $RbCs_{11}O_3$ has been solved in the meantime;[18] single-crystal data of another phase not yet evaluated definitely prove the existence of $Rb_2Cs_{11}O_3$.[19] The investigations are extremely difficult due to nonequilibrium effects in this part of the ternary system. This behavior too resembles the characteristic difficulties with the preparation of Cs_4O due to the kinetics of crystallization.[7]

Deviation from the Stoichiometry $Rb_7Cs_{11}O_3$. Samples of different compositions containing $Rb_7Cs_{11}O_3$ have been prepared repeatedly. In the corresponding Guinier diagrams significant line shifts of the compound patterns indicate a range of homogeneity. To learn about the nature of the deviations in stoichiometry of this first metal mixed suboxide, a variety of samples with compositions near the exact stoichiometry have been investigated leading to the following results.

(a) According to the Guinier diagrams, a broad range of homogeneity exists along the line of constant oxidation number in the ternary system defined by the sample compositions $(Rb_xCs_{1-x})_6O$. Preliminary results clearly reveal a homogeneous phase within the $Cs_{13}Rb_5O_3$ and $Cs_6Rb_{12}O_3$ limits according to x-ray investigations of selected samples along this line of compositions. The exact phase width has yet to be determined by further experiments.

With respect to the crystal structure, the range of homogeneity is well understood. Samples within the triangle between Rb, Cs, and $Cs_{11}O_3$ of the ternary system contain pure $Cs_{11}O_3$ clusters. The range of homogeneity of $Rb_7Cs_{11}O_3$ results from a substitution of Rb atoms in the metallic parts of the structure according to the formula $Rb_{7-x}Cs_{11}O_3$. A similar replacement has been found with Cs_7O ($Cs_{10}Cs_{11}O_3$),[6] where Cs atoms in the oxygen-free part of the structure can partly be replaced by Rb atoms. As soon as one passes the borderline of composition $Rb_xCs_{11}O_3$, the substitution of Cs atoms by Rb atoms occurs. On the right-hand side of this line the range of homogeneity is caused by a metal substitution in the ionic parts of the structure according to $Rb_7Cs_{11-x}Rb_xO_3$. As a consequence $Rb_7Cs_{11}O_3$ itself has to be formulated as $Cs_xRb_{7-x}Cs_{11-x}Rb_xO_3$. But there is no experimental evidence for a mutual replacement of Rb and Cs with the exact compound composition. An internal redox reaction leads to the pure $Cs_{11}O_3$ cluster in this case.

(b) Investigations along the line of compositions $Rb_xCs_{11}O_3$ yield no indication of deviation from the stoichiometry $Rb_7Cs_{11}O_3$ in this special direction of the ternary system. Thus

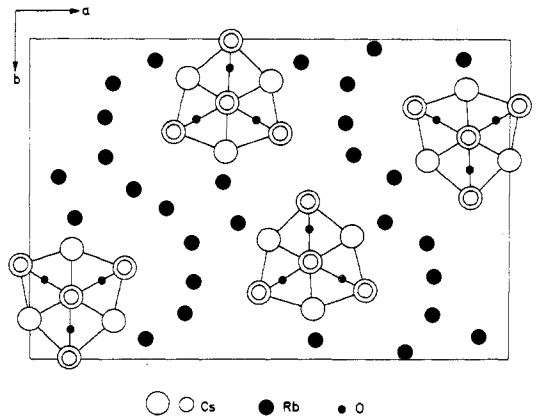

Figure 4. Projection of the structure of $Rb_7Cs_{11}O_3$ along [001].

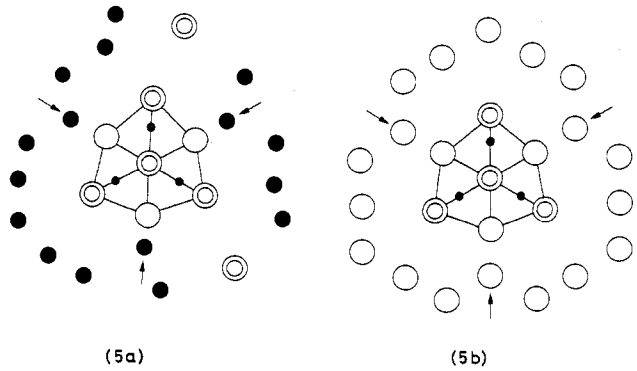

Figure 5. Comparison of the atomic environment of the $Cs_{11}O_3$ cluster in (a) $Rb_7Cs_{11}O_3$ and (b) $Cs_{10}Cs_{11}O_3$ (Cs_7O). Representation of atoms as with Figure 4.

the "intercalation" of metal atoms between $Cs_{11}O_3$ clusters happens to occur strictly in the stoichiometric ratio 7:1. Obviously (as with the metal-rich binary suboxides) geometrical factors are responsible for the well-defined cluster-to-metal atom ratio.

Structure Description and Discussion

The structure of $Rb_7Cs_{11}O_3$ is drawn as a projection along [001] in Figure 4. The atomic arrangement clearly demonstrates the unusual fact that the chemically very similar metals rubidium and cesium are structurally entirely separated in this compound. Table I comprises the atomic parameters including the refined occupation factors. Within the accuracy of the structure determination no indication of a mutual replacement of Rb and Cs atoms is observed.

The structure contains the characteristic trigonal $Cs_{11}O_3$ clusters, which are the same as in the binary compounds $Cs_{11}O_3$, Cs_4O, and Cs_7O. They are formed by face sharing of three equivalent coordination octahedra of Cs atoms around the oxygen atoms. According to the different coordination numbers 1, 2, and 3 of the Cs atoms toward oxygen, the interatomic distances are as follows (see Table II): d(III–III) = 371 (369), d(III–II) = 374 (376), d(III–I) = 414 (415), d(II–I) = 427 (429), and d(I–I) = 402 (405) pm. The numbers in parentheses refer to the corresponding averaged distances in the binary cesium compounds. They demonstrate the identity of the clusters in all of the compounds, even when geometrical details are concerned. The same holds for the Cs–O distances: d(O–III) = 296 (296), d(O–II) = 290 (291), and d(O–I) = 273 (273) pm. The interatomic distances clearly reflect the ionic type of bonding in the clusters—the Cs–Cs as well as the Cs–O distances correspond to the distances in Cs_2O (382, 419, 426, and 286 pm, respectively).[20] The nearest-neighbor distances between the Rb atoms (as well as the contact distances between the $Cs_{11}O_3$ clusters) are comparable to the M–M distances in metallic Rb (490 pm at −50 °C[5]) and Cs (531 pm at −50 °C[9]). Thus the Rb atoms constitute the purely metallic parts of the structure. They mainly belong to wavy planes of close-packed atoms perpendicular to [100] filling the space between the $Cs_{11}O_3$ clusters.

Both the arrangement of clusters and their surrounding by metal atoms in $Rb_7Cs_{11}O_3$ exhibit striking similarities to the characteristic features of the crystal structure of Cs_7O ($Cs_{10}Cs_{11}O_3$) as is demonstrated in Figure 5. In both compounds the $Cs_{11}O_3$ clusters are arranged in columns and the threefold axis of the clusters coincides with the column axis. In spite of the different structures, these columns are surrounded by metal atoms in very much the same way. Three of the surrounding atoms are of special importance with respect to the stabilization of the threefold symmetry of cluster columns. These atoms (marked by arrows in Figure 5) fit into the gaps between adjacent clusters. In the compounds $Cs_{11}O_3Cs$ and $Cs_{11}O_3$ themselves the metal atom-to-cluster ratio is smaller than 3:1. Since there is no stabilization, the

Table II. Interatomic Distances (pm) in $Rb_7Cs_{11}O_3$ below 570 pm (Standard Deviations in Parentheses)[a]

Distances in the $Cs_{11}O_3$ Cluster	
	Cs–Cs
I–I: 3–4, 5–6, 7–8	399.5 (23), 405.0 (18), 402.8 (20)
II–I: 9–3, –4, –5, –6	426.5 (20), 430.2 (21), 427.2 (18), 431.0 (17)
10–5, –6, –7, –8	424.1 (15), 431.4 (16), 423.6 (16), 429.2 (15)
11–3, –4, –7, –8	424.9 (19), 424.6 (20), 426.9 (19), 429.2 (18)
III–I: 1–3, –5, –7	417.1 (15), 410.4 (18), 407.6 (18)
2–4, –6, –8	412.0 (15), 419.3 (18), 416.4 (18)
III–II: 1–9, –10, –11	327.8 (16), 372.7 (12), 376.1 (15)
2–9, –10, –11	373.3 (16), 377.4 (12), 372.4 (15)
III–III: 1–2	371.0 (13)
	Cs–O
I–O: 3–1, 4–1, 5–2	262.7 (87), 287.6 (96), 263.1 (91)
6–2, 7–3, 8–3	269.4 (90), 270.8 (67), 283.1 (67)
II–O: 9–1, 2, 10–2, –3	306.6 (46), 287.7 (50), 296.5 (50), 284.3 (34)
11–1, –3	270.3 (46), 292.8 (34)
III–O: 1–1, –2, –3	286.1 (77), 303.0 (78), 285.1 (60)
2–1, –2, –3	301.4 (85), 306.4 (78), 293.0 (62)
Distances between $Cs_{11}O_3$ Clusters and Rb Atoms	
	Cs–Cs
1–2′; 3–4′, –7′	533.1 (14), 504.7 (23), 511.8 (21)
4–8′, 5–6′, 7–8′	505.1 (20), 499.2 (18), 501.5 (20)
	Cs–Rb
3–1, –7; 4–1, –7	504.8 (24), 556.7 (22), 502.4 (24), 547.7 (23)
5–1, –2, –3, –4, –5	558.3 (20), 567.0 (18), 551.9 (19), 538.7 (21), 529.5 (19)
6–1, –2, –3, –4, –5, –6	557.5 (20), 566.8 (17), 552.6 (18), 535.5 (20), 521.8 (19), 533.8 (24)
7–4, –7; 8–4, –6, –7	555.2 (21), 565.1 (20), 556.4 (21), 509.7 (24), 569.5 (20)
9–1, –3, –3′, –3″	498.4 (11), 514.6 (28), 514.8 (28), 499.2 (11)
10–2, –4, –4′, –7	569.0 (10), 497.9 (28), 500.1 (28), 503.9 (10)
11–4, –5, –7, –7′	512.7 (11), 509.4 (12), 505.6 (26), 510.5 (26)
	Rb–Rb
1–3, –3′, –3″, –5, –6	551.7 (33), 548.9 (33), 508.8 (13), 494.3 (13), 509.4 (44)
2–5, –5′, –7	539.1 (12), 548.2 (33), 506.2 (13)
3–3′, –6; 4–5, –7	549.9 (27), 496.1 (13), 470.7 (14), 542.1 (30)
5–6	527.1 (41)

[a] Roman numerals denote coordination number toward oxygen, arabic numbers refer to Table I.

clusters within the columns are inclined. The different sizes of Rb and Cs atoms are clearly expressed by two facts: First, the atoms marked by arrows are shifted toward the center of the cluster column (into the gaps) in the case of Rb. Second, in spite of this shift, the identity period of the column is slightly smaller in $Rb_7Cs_{11}O_3$ (903 pm as compared to 915 pm in Cs_7O at −50 °C[6]).

As in the case of $Rb_7Cs_{11}O_3$, the number of Rb atoms per cluster is too small to occupy all possible metal atom positions around the cluster. Cs atoms of the neighboring clusters replace the missing Rb atoms (see Figure 5). Since the clusters are comparably rigid, this substitution leads to distortions in the neighborhood of the columns in $Rb_7Cs_{11}O_3$ as compared to Cs_7O. Except for such distortions the arrangements of atoms around the $Cs_{11}O_3$ clusters are principally identical in all compounds containing this type of cluster, even in $Cs_{11}O_3$ itself where all surrounding atoms belong to neighboring clusters. These nearly identical geometrical features—despite very different compound compositions and crystal structures—lead to the conclusion that the special packing of clusters (and single metal atoms) is an essential factor determining the cluster-to-metal atom ratio in alkali metal suboxides and thus determining the stoichiometries of the existing compounds. The metallic bonds between the clusters and the intermediate single atoms call for a high space filling. This principle is difficult to recognize in the case of the $Cs_{11}O_3$ cluster, as the Cs atoms of this cluster are not arranged in a way to constitute a part of (an infinitely) close-packed array of spheres. Therefore the close-packed principle with $Cs_{11}O_3$ clusters is not as obvious as in the case of Rb_9O_2 clusters, where all atoms belong to a (infinitely) close-packed arrangement.

Besides the analytical and structural investigations, measurements have been carried out with respect to the electronic properties of $Rb_7Cs_{11}O_3$. Especially photoelectron spectroscopy (UV PES) leads to results,[21] which are only partly understood on the basis of the formula and structure of $Rb_7Cs_{11}O_3$.

The excitation by He I radiation ($h\nu$ = 21.2 eV) yields photoemission from the conduction band, the very sharp O 2p level (binding energy with respect to the Fermi level 2.7 eV), the Cs $5p_{3/2,1/2}$ levels (11.5, 13.1 eV), and the corresponding Rb 4p levels (15.3, 16.2 eV). All structures are clearly resolved. The binding energies of the Rb 4p states are the same as in metallic Rb, whereas the energies of the Cs 5p states are lowered from 12.1 and 14.0 eV in the metal to nearly the same values as with $Cs_{11}O_3$.

The partly filled conduction band as well as the occurrence of energy loss structures due to the excitation of surface plasmons reveal the metallic nature of $Rb_7Cs_{11}O_3$. This qualitative result agrees with the idea of chemical bonding in $Rb_7Cs_{11}O_3$ (as well as the other alkali metal suboxides). But a quantitative determination of the free electron concentration N from the observed value of the surface plasmon energy $\hbar\omega_{sp}$ leads to a result which is not yet understood. Details of the calculation are given elsewhere.[21] Using the relationship $\hbar\omega_{sp}$ = (constant)N, together with the structural data of $Rb_7Cs_{11}O_3$, one calculates a number of 7 free electrons per formula unit. This number is much too low, as one would expect 12 electrons per formula unit with the assumption that $Rb_7Cs_{11}O_3$ contains Rb^+ and Cs^+ ions (as in the pure metals) besides O^{2-} ions. In the case of binary suboxides ($Cs_{11}O_3$ and $Cs_{10}Cs_{11}O_3$) the experimental values are nearly equal to the expected ones (5 and 15, respectively). The special situation with $Rb_7Cs_{11}O_3$ is reflected in the electrical resistivity of this compound, too. Resistivity measurements have been performed on all alkali metal suboxides using a simple contactless eddy current method.[22] Besides the very low residual resistivity ratio ρ(250 K):ρ(4 K) ≈ 3 in the case of $Rb_7Cs_{11}O_3$ (in contrast to $rrr \approx$ 200 with, e.g., $Cs_{10}Cs_{11}O_3$) due to its nonstoichiometric nature, the specific resistivity of $Rb_7Cs_{11}O_3$ is a factor of 2 higher than with the binary suboxides even when the low-temperature residual has been subtracted.[23] The low conductivity possibly due to a low carrier concentration cannot be explained on the basis of the broad range of homogeneity of $Rb_7Cs_{11}O_3$, as the stoichiometry M_6O (thus the electron concentration) is preserved in the homogeneous phase. We hope to find an explanation for this discrepancy (possibly due to scattering or trapping of electrons in the mixed-metal suboxide) by investigating the phases $(Cs,Rb)_{10}Cs_{11}O_3$,[19] $[(Cs,Rb)_{11}O_3](Cs,Rb)_7$, and $(Cs,Rb)_{11}O_3$.[18]

Registry No. $Rb_7Cs_{11}O_3$, 60937-26-0.

Supplementary Material Available: A listing of observed and calculated structure factor amplitudes (4 pages). Ordering information is given on any current masthead page.

References and Notes

(1) A. Simon, "Crystal Structure and Chemical Bonding in Inorganic Chemistry", C. J. M. Rooymans and A. Rabenau, Ed., North-Holland Publishing Co., Amsterdam, 1975, p 47.
(2) A. Simon, "Homoatomic Rings and Chains and Macromolecules of Main Group Elements" A. Rheingold, Ed., Elsevier, Amsterdam, Oxford, New York, 1977, p 117.
(3) A. Simon, *Naturwissenschaften*, **58**, 623 (1971); *Z. Anorg. Allg. Chem.*, **431** (1977).
(4) A. Simon and E. Westerbeck, *Z. Anorg. Allg. Chem.*, **428**, 187 (1977).
(5) A. Simon and H.-J. Deiseroth, *Rev. Chim. Miner.*, **13**, 98 (1976).
(6) A. Simon, *Z. Anorg. Allg. Chem.*, **422**, 208 (1976).
(7) A. Simon, H.-J. Deiseroth, E. Westerbeck, and B. Hillenkötter, *Z. Anorg. Allg. Chem.*, **423**, 203 (1976).
(8) W. Brämer, Thesis, Münster, 1975.
(9) A. Simon, W. Brämer, B. Hillenkötter, and H.-J. Kullmann, *Z. Anorg. Allg. Chem.*, **419**, 253 (1976).
(10) A. Simon, *Z. Anorg. Allg. Chem.*, **395**, 301 (1973).
(11) R. H. Purcell, *J. Chem. Soc.*, 1207 (1928).
(12) A. Simon, *J. Appl. Crystallogr.*, **3**, 11 (1970); **4**, 138 (1971).
(13) H. W. King and C. M. Russell, *Adv. X-Ray Anal.*, **10**, 354 (1967).
(14) J. Taylor, M. Mack, and W. Parrish, *Acta Crystallogr.*, **17**, 1229 (1964).
(15) J. M. Stewart, G. J. Kruger, H. L. Ammon, C. Dickinson, and S. R. Hall, "The X-Ray System 1972", Computer-Science Center, University of Maryland.
(16) Landoldt-Börnstein, "Atom- und Molekularphysik", Vol. I, Part 1, Springer-Verlag, West Berlin and Heidelberg, 1950, p 211.
(17) E. Westerbeck, Diplomarbeit, Münster, 1971.
(18) H.-J. Deiseroth and A. Simon, to be submitted for publication.
(19) A. Simon and W. Brämer, to be submitted for publication.
(20) K.-R. Tsai, P. M. Harris, and E. N. Lassettre, *J. Phys. Chem.*, **60**, 338 (1956).
(21) G. Ebbinghaus, W. Braun, and A. Simon, *Z. Naturforsch., B*, **31**, 1219 (1976).
(22) W. Bauhofer, *J. Sci. Instrum.*, in press.
(23) W. Bauhofer and A. Simon, unpublished results, 1976.